PROCEEDINGS OF SPIE

SPIEDigitalLibrary.org/conference-proceedings-of-spie

Non-destructive testing of graphene/ epoxy composites using THz waves

Magnus W. Haakestad, Bernt B. Johnsen, Anh Hoang Dam, Johann Mastin, Michel Eid, et al.

Magnus W. Haakestad, Bernt B. Johnsen, Anh Hoang Dam, Johann Mastin, Michel Eid, Arthur D. van Rheenen, "Non-destructive testing of graphene/ epoxy composites using THz waves," Proc. SPIE 10800, Millimetre Wave and Terahertz Sensors and Technology XI, 108000A (5 October 2018); doi: 10.1117/12.2325539

SPIE.

Event: SPIE Security + Defence, 2018, Berlin, Germany

Non-destructive testing of graphene/epoxy composites using THz waves

Magnus W. Haakestad[a], Bernt B. Johnsen[a], Anh Hoang Dam[b], Johann Mastin[b], Michel Eid[b], Arthur D. van Rheenen*[a]

[a]Norwegian Defence Research Establishment (FFI), P. O. Box 25, NO-2027 Kjeller, Norway;

[b]CealTech AS, Postboks 91, 4064 Stavanger, Norway

*arthur-d.vanrheenen@ffi.no

ABSTRACT

In earlier experiments [1] we found there was significant transmission of THz radiation through carbon-fiber enforced composites, despite that fact that the dc conductivity of the carbon fibers is expected to be good and hence should prevent penetration of electro-magnetic radiation. To study the relationship between absorption of THz radiation and electrical conductivity we performed measurements on samples with different concentrations of graphene in an epoxy matrix. We observed an increased absorption of THz radiation with increased graphene concentration. Our conductivity measurements (simple transverse DC measurements using tin foil as electrodes that cover the two sample surfaces) showed the typical increase of several orders of magnitude with graphene concentration. Although both the conductivity and the THz absorption increase with graphene concentration, there is no direct cause-and-effect relation between the two quantities. Careful analysis shows that even the highest dc conductivity values cannot explain even the lowest observed values for the THz absorption coefficient.

Keywords: THz transmission, THz absorption, graphene, dielectric properties, electrical conductivity, epoxy, non-destructive testing

1. INTRODUCTION

Graphene has many attractive properties: it is a very light and very strong material, and it conducts both heat and electricity very well. Thus, it could possibly be integrated into many materials systems, enhancing their performance. Since Geim and Novolosev discovered the so-called “Scotch-tape” method, a mechanical exfoliation technique, to extract thin flakes of graphene from graphite in 2004, the number of graphene-research publications has roughly doubled every 2 years [2]. The simple extraction technique made the material widely available, albeit in small quantities, and combined with the very promising properties the interest in the field grew enormously. Some of the applications that have emerged (are foreseen) are: transparent electrodes in solar cells [3], data storage [4], high-speed electronics, even though the lack of a bandgap is a setback that could possibly be alleviated by developing derivatives [5-7], smart window and displays [8-9], and supercapacitors [10-16]. These applications are all well described in Reference 17. The strength and light weight of the material may be leveraged in for instance body armor or airplane components. One final application we like to mention is using graphene as a microwave-absorbing material protecting sensitive electronic equipment [18]. In this paper we report on our investigation of the THz absorbance of graphene/epoxy compounds and look into a possible relationship with the electrical conductivity of the compound. After describing the details of the fabrication process of the samples used in this study, we present the THz measurement technique and the results from these measurements, followed by a description of the measurement technique of the electrical conductivity as well as the results we obtained. Next, we discuss the results, investigating the possibility to correlate the observed absorbance with the dc conductivity and the result of this investigation is reiterated in the Conclusions section.

Millimetre Wave and Terahertz Sensors and Technology XI, edited by Neil A. Salmon, Frank Gumbmann, Proc. of SPIE Vol. 10800, 108000A · © 2018 SPIE
CCC code: 0277-786X/18/$18 · doi: 10.1117/12.2325539

2. GRAPHENE/EPOXY COMPOSITE SAMPLES

Samples of neat epoxy polymer and graphene/epoxy composites were prepared. The neat epoxy sample was included as a reference.

The neat epoxy polymer samples were prepared by mixing Araldite LY 556 epoxy resin, Aradur 917 hardener, and Accelerator DY 070 at the weight ratio 100:90:1. The blend was mixed manually, heated to 60 ^{o}C, and then mixed thoroughly again. The blend was then cast in aluminum cups that had been coated with a release agent. The employed curing cycle was 4 hours at 80 ^{o}C and 8 hours at 140 ^{o}C. The size of the cured samples was around 41 mm in diameter and 1-2 mm in thickness.

For preparation of cured graphene/epoxy samples, master batches of graphene in the epoxy resin (Araldite LY 556) or the hardener (Aradur 917), were employed. The master batches were prepared by CealTech AS using their proprietary methods to ensure stable and homogeneous dispersion at various graphene concentrations (up to 16 wt. %). A solvent-based method was employed to disperse a commercial graphene powder into the epoxy resin or hardener. The solvent helps the polymer chains to intercalate in-between the graphene sheets and exfoliate the sheets while dispersing them. The solvent was subsequently removed, leading to the formation of graphene/epoxy and graphene/hardener master batches. The master batches were employed to prepare the graphene/epoxy samples, which are listed in Table 1. From a single master batch several samples with different concentrations were prepared by proper dilution, and from each of these concentrations two, sometimes three samples with different thicknesses were formed. For instance, master batch S3 (see sample ID in column 2 of the table) was used to make four concentrations: 0.42, 0.28, 0.24, and 0.07 wt,% graphene, resulting in a total of eight samples: numbers 3 – 10.

The graphene/epoxy samples were prepared in a similar manner to the neat epoxy samples, making sure that the mixing ratio of the polymer components was correct. However, the graphene master batches were highly viscous. To lower the viscosity during processing, they were heated to 60 ^{o}C prior to mixing. Using this method, graphene/epoxy samples with graphene concentration up to 12 wt. % could be fabricated. The cured samples seemed to be free of voids by visual inspection.

The fabricated samples, 52 in total, were subsequently characterized in terms of electrical conductivity and THz transmission.

Table.1 Overview of the compositions of the graphene/epoxy samples. The samples were disks with ~41 mm diameter and 1-2 mm thickness. Master batches S3-S5 were dispersions of graphene in epoxy and master batch S8 was graphene in hardener.

Sample number	Master batch	Graphene content in master batch (wt. %)	Graphene content in sample (wt. %)
1-2	n/a	0.0	0.00
3-4	S3	0.8	0.42
5-6	S3	0.8	0.28
7-8	S3	0.8	0.14
9-10	S3	0.8	0.07
11-12	S4	4.0	0.42
13-14	S5	8.0	0.42
15-17	S4	4.0	0.14
18-20	S4	4.0	0.84
21-23	S4	4.0	1.26
24-26	S4	4.0	2.10
27-29	S5	8.0	0.14
30-32	S5	8.0	0.84
33-35	S5	8.0	1.26

36-38	S5	8.0	2.10
39-41	S5	8.0	2.94
42-44	S5	8.0	4.20
45-46	*S8*	*16.0*	*4.20*
47-48	*S8*	*16.0*	*6.22*
49-50	*S8*	*16.0*	*8.24*
51-52	*S5/S8*	*8.0/16.0*	*11.92*

The graphene powder used in this study was obtained from a commercial supplier and some of the properties of the graphene are listed in Table 2.

Table 2. Some properties of the graphene powder

Average thickness:	10-20 nm
Average transverse dimension:	5 µm
Specific surface area:	≥ 15 m^2/g
True density:	≤ 2.20 g/cm^3
Solids:	$\geq 98.80\%$
Moisture:	$\leq 1.20\%$
Carbon content:	$\geq 95.00\%$
Oxygen content:	$\leq 4.00\%$
Hydrogen content:	$\leq 1.00\%$
Nitrogen content:	$\leq 0.20\%$
Ash content:	$\leq 2.50\%$

Figure 1 shows examples of two prepared samples: the neat epoxy sample and an example of a graphene/epoxy sample.

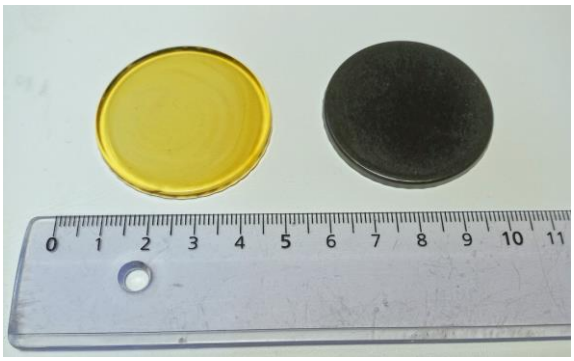

Figure 1. Examples of a neat epoxy sample (left) and a graphene/epoxy composite sample (right).

3. THZ MEASUREMENTS

3.1 Set-up

The THz setup, schematically shown in Figure 2, is based on a fiber-coupled time-domain spectroscopy system pumped by 100-fs pulses at 780 nm wavelength from a frequency-doubled Er-doped fiber laser [19]. It is driven by a femtosecond laser that emits 120-fs-long pulses at a wavelength of about 1.55 μm. The wavelength of the pulses is halved (frequency doubling) using a nonlinear crystal, the power is split 50/50 and one-half of this power then illuminates the emitter. This is a piece of low-temperature grown GaAs where the incoming laser light pulses create electron-hole pairs that are accelerated in an applied electric field and in the process emit electromagnetic radiation that mainly covers the THz frequency domain. The frequency doubling of the laser light is necessary to excite electrons above the GaAs bandgap. The repetition rate of the laser is 90 MHz. The THz radiation is pointed to a sample and a detector measures transmitted THz radiation. The detection principle is the inverse of the generation principle. The other half of the original laser light power is diverted through a variable delay line and shone on the detector to create electron-hole pairs and prepare the detector for reception of the THz radiation. The E-field from the THz pulse produces then a tiny current in the detector, which is detected by a lock-in amplifier. One then steps through the detected pulse by adjusting the delay line and in this way builds up the transmitted or reflected THz wave, measuring the THz E-field as a function of time. Fiber coupling of the laser light into the measurement heads allows for flexible placement of detector end emitter with respect to the sample [19]. Figure 3 shows typical reference and noise spectra.

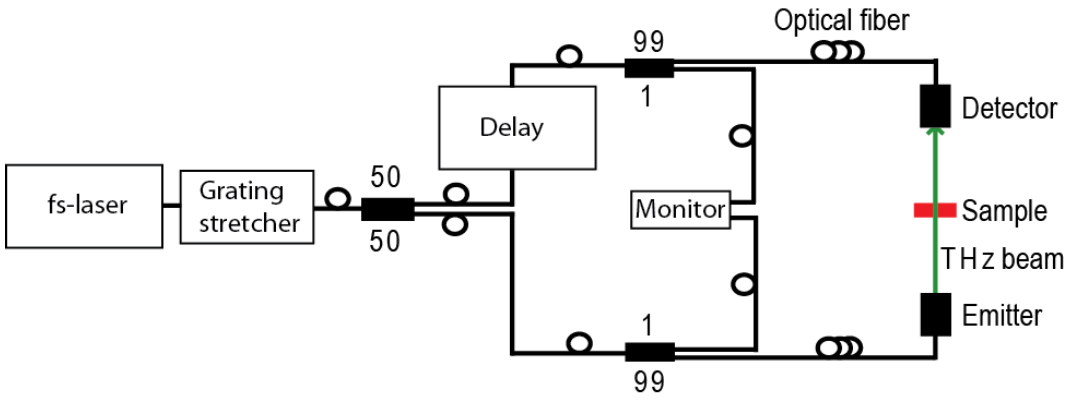

Figure 2. Schematic overview of the fiber-coupled THz-TDS system configured in transmission mode [1].

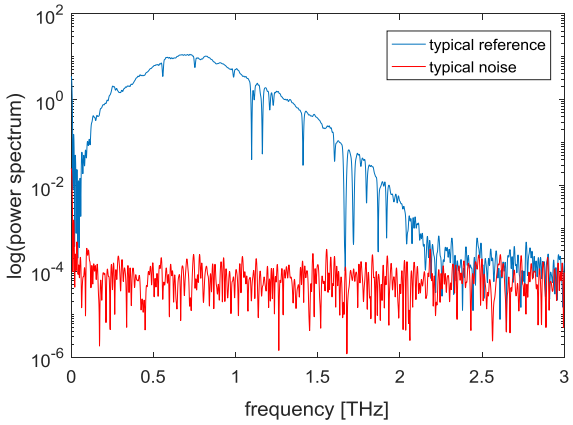

Figure 3. Typical reference and noise spectra for the set-up in Fig. 2. Typically the maximum SNR > 60 dB and the bandwidth > 2.0 THz

3.2 THz absorption coefficient

The transmission measurements are performed by measuring the THz amplitude with and without a sample present and averaging over a large number of pulses to improve the signal-to-noise ratio. By considering the transmission of plane electromagnetic waves through a slab at normal incidence, one can derive an expression for the transmission coefficient. See Figure 4 for a sketch of the transmitted and reflected waves, the basis for the analysis. When neglecting multiple reflections in the sample, assuming that air has a refractive index of 1, and assuming that there are no strong absorption lines, such that the imaginary part of the index of refraction, Im *n*, is much less than the real part, Re *n*, we find that

$$\frac{E_s(\omega)}{E_r(\omega)} \approx \frac{4\,\mathrm{Re}\,n}{(\mathrm{Re}\,n+1)^2}\exp\left[i\omega(n-1)L/c\right] \tag{1}$$

where $E_s(\omega)$ and $E_r(\omega)$ are the Fourier transform of the measured temporal THz amplitude with and without sample, respectively. *L* is the sample thickness, ω is the angular frequency, and *c* is the vacuum speed of light. From Eq. (1), we obtain

$$\mathrm{Re}\,n = \frac{c}{\omega L}\,\mathrm{Im}\left[\ln\left(\frac{E_s(\omega)}{E_r(\omega)}\right)\right]+1 \tag{2}$$

and

$$\mathrm{Im}\,n = \frac{c}{\omega L}\left\{\ln\left[\frac{4\,\mathrm{Re}\,n}{(\mathrm{Re}\,n+1)^2}\right]-\mathrm{Re}\left[\ln\left(\frac{E_s(\omega)}{E_r(\omega)}\right)\right]\right\} \tag{3}$$

The relation between Im *n* and the power absorption coefficient, α, is given by

$$\alpha = \frac{2\omega}{c}\,\mathrm{Im}\,n \tag{4}$$

In essence, Im *n* denotes the absorption per wavelength, while α is the absorption per length unit. Note that Im $n > 0$ for $\omega > 0$ for any passive medium, i.e. a passive medium is always lossy. A retrieved Im $n < 0$ is unphysical and indicates uncertainties in the measurement results. One essential point with Eq. (3) is that it takes into account Fresnel reflection at the sample boundary, in order to get the intrinsic absorption coefficient of the sample.

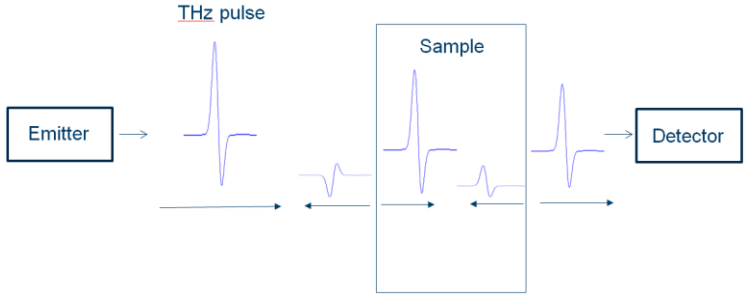

Figure 4. Measurement geometry for transmission mode. Note the emitted and reflected pulse on the emitter side of the sample and the transmitted pulse on the detector side.

3.3 Measurement results

Terahertz transmission measurements were carried out in ambient air using the set-up in Fig. 2. No smoothing was applied to the spectra and water vapor lines were not removed. Example spectra are shown in Fig. 5.

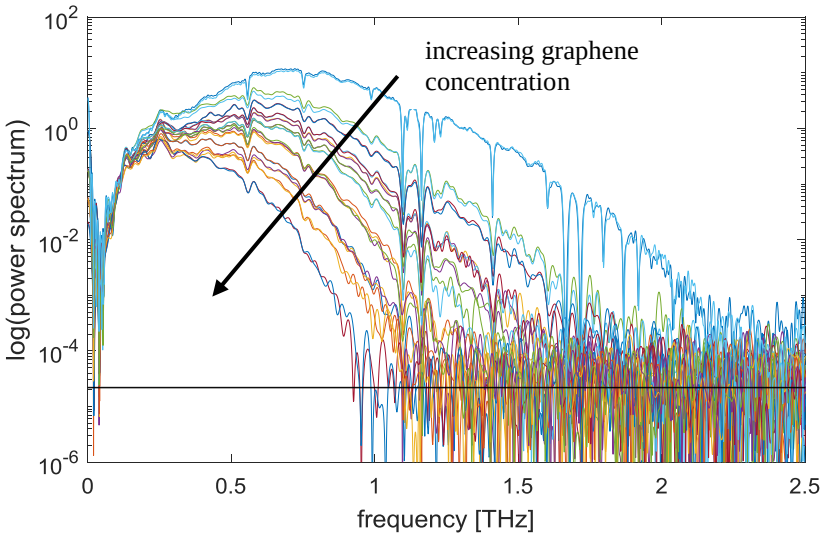

Figure 5. Examples of measured transmission spectra. Bandwidth and signal strength are reduced with increasing graphene concentration. Also, apart from the water vapor absorption lines, there are no spectral features.

We observe that increased graphene concentration causes a broad-band increase in absorption (reduced transmission) and we do not observe absorption lines due to the graphene. The absorption lines in the spectrum are associated with water vapor. No smoothing is applied when calculating the spectra from the time traces.

The absorption coefficient of the samples was extracted using Eq. (4) and the real part of the refractive index was determined using Eq. (2). Example of the absorption spectra for some samples are presented in Fig. 6

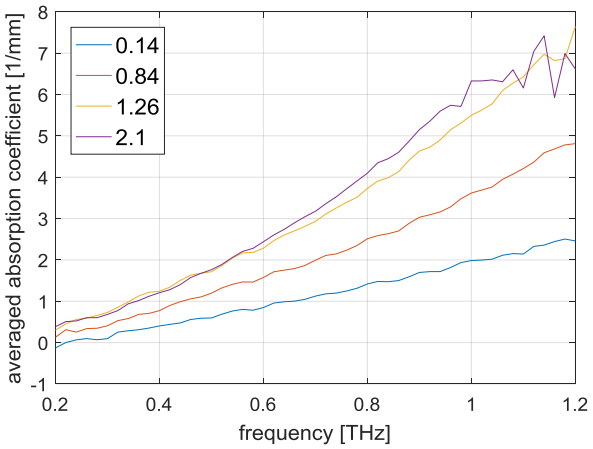

Figure 6. Examples of averaged (over sample thicknesses) absorption coefficient. The legend indicates the graphene concentration, wt-%.

Figure 6 shows again that typically the broad-band absorption increases with increased graphene concentration and the spectra are relatively smooth without any absorption lines.

Both the real part of the refractive index and the absorption coefficient depend on frequency, but the results are reported here at a frequency at 0.3 THz, because this was the highest frequency that gave a good signal for all samples, and because no significant spectral features were observed in the spectra about this frequency. Figure 7 shows the measured absorption coefficient for the different samples. It is clear from the figure that the absorption coefficient increases with increasing graphene concentration. Note that one of the measurements at 0 wt. % graphene concentration (i.e. neat epoxy) shows negative absorption, but this is unphysical and represents the typical measurement uncertainty. The different symbols represent the different master batches from which the samples were produced.

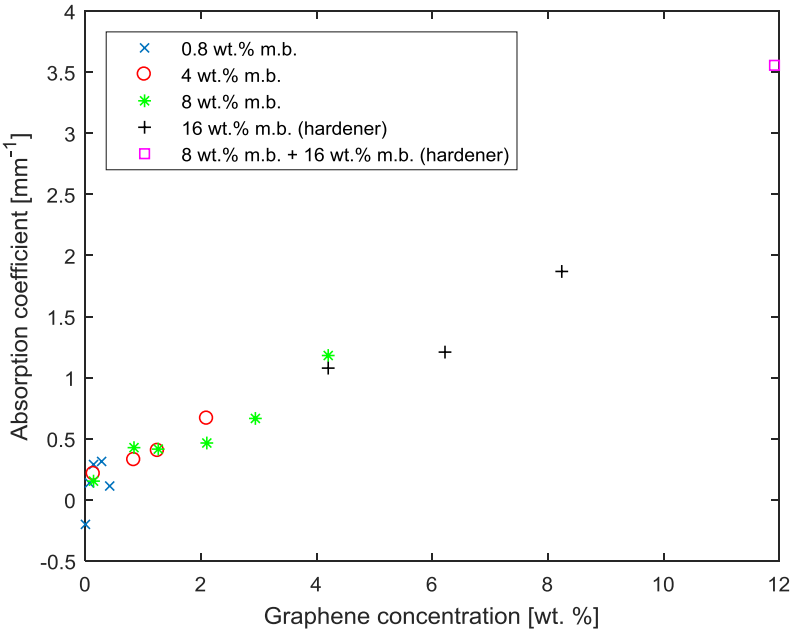

Figure 7. Measured absorption coefficient at a frequency of 0.3 THz as a function of graphene concentration for the different samples. Fresnel reflection at the sample interfaces is corrected for. The different symbols represent the different master batches (m. b.) from which the samples were produced.

The real part of the measured refractive index at 0.3 THz is shown in Fig. 8. It is apparent from the figure that the real part of the refractive index also increases with increasing graphene concentration. An increase in Re *n* implies an increase in the optical path length through the sample. This manifested itself as an increase in the propagation delay of the THz pulses through the samples as the graphene concentration increased.

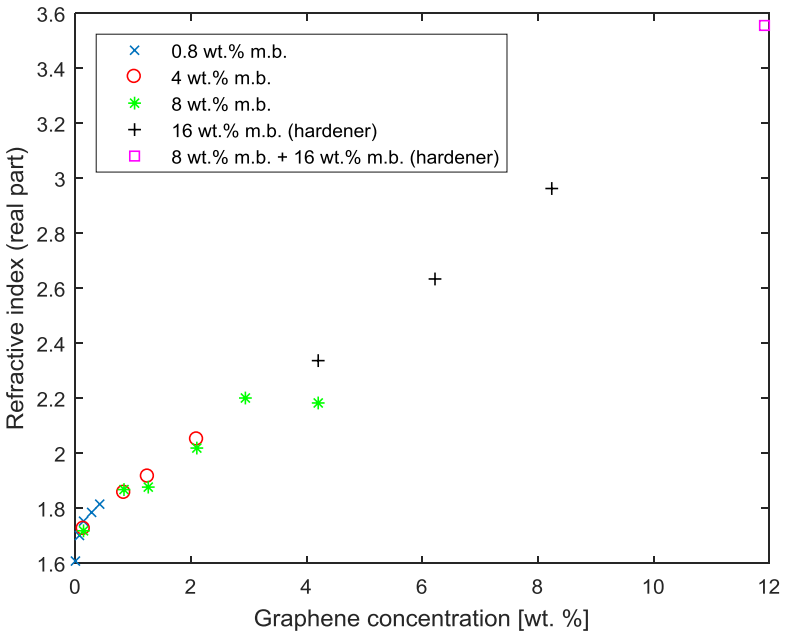

Figure 8. Measured real part of the refractive index at a frequency of 0.3 THz as a function of graphene concentration for the different samples. The different symbols represent the different master batches (m. b.) from which the samples were produced.

4. ELECTRICAL CONDUCTIVITY MEASUREMENTS

We measured the dc conductance of the samples perpendicular to the circular surfaces. In order to ascertain good contact, the surfaces contact areas were covered with tin foil between two large area electrodes placed in a vise. A Keithley 236 Source Measure Unit was used to be able to generate the relatively large required voltages and measure the small currents. A sketch of the set-up is shown in Fig. 9.

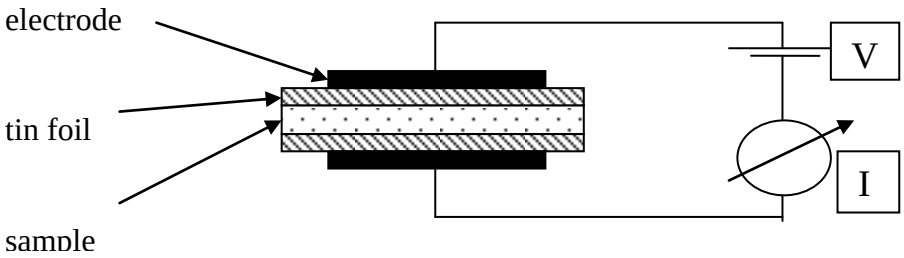

Figure 9. Setup for measurement of electrical conductivity. The sample to be tested is placed between two electrodes, which are pressed onto the sample using a vise. The current through the sample is measured as a function of applied voltage.

The voltage V is ramped up and the current I through the sample is measured. The (I, V) data are fitted to a straight line and the electrical conductivity, σ, is calculated from the slope:

$$\sigma \approx \frac{L}{A}\frac{I}{V}. \tag{5}$$

In this expression L is the thickness of the sample and A is the contact area.

Figure 10 shows the measured electrical conductivity as a function of graphene concentration for all samples listed in Table 1. We observe that the conductivity is of the order of 10^{-12} S/m for the lowest graphene concentrations, while it increases to 10^{-5} S/m for the highest graphene concentration. The latter is still a low conductivity, and it corresponds to a measured resistance of about 100 kΩ through the sample. We further observe that there is good correspondence between graphene concentration and conductivity, also for samples with the same wt. % but produced from different master batches (m.b.), except for the samples prepared from the master batch with 16 wt. % graphene in hardener (+ symbol).

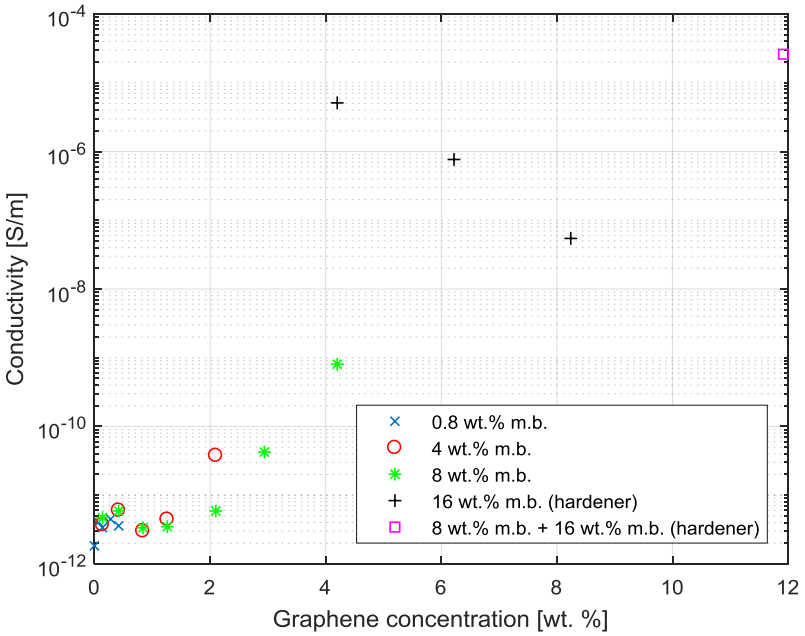

Figure 10. Measured electrical conductivity as a function of graphene concentration for the different samples. The symbols correspond to the master batches (m.b.) from which they are produced.

5. DISCUSSION OF RESULTS

We observed that both the absorption coefficient and the electrical conductivity increase with increased concentration of dispersed epoxy. For low concentrations of graphene the conductivity is low (~10^{-12} S/m) and then rises rapidly, orders of magnitude, as the concentration increases. The absorption coefficient increases with graphene concentration as well, but at a more moderate pace. The question arises naturally whether the observed absorption coefficient may be explained by the electrical conductivity. To investigate this we start off by considering one of Maxwell's equations for a lossy medium:

$$\nabla \times \vec{H} = -i\omega\varepsilon_0 \left(\varepsilon + \frac{i\sigma}{\omega\varepsilon_0} \right) \vec{E}, \tag{6}$$

where we define an effective permittivity

$$\varepsilon_{eff} = \varepsilon + \frac{i\sigma}{\omega\varepsilon_0}. \tag{7}$$

The relative permittivity and the refractive index are related according to $n_{\text{eff}} = \varepsilon_{\text{eff}}^{1/2}$.

Using algebra we find

$$\alpha = \frac{2\omega}{c}\mathrm{Im}(n) = \frac{\sigma}{c\varepsilon_0\,\mathrm{Re}(n)} \tag{8}$$

With $\sigma = 10^{-5}$ S/m (the highest conductivity value we measured) and Re(n) = 1.7, we find $\alpha = 2\times10^{-6}$ mm^{-1}. This value for the absorption coefficient is several orders of magnitude smaller than the measured absorption coefficient values. We conclude therefore, that the electrical conductivity of the samples has a negligible contribution to the absorption coefficient.

6. CONCLUSIONS

In conclusion, we have fabricated epoxy samples with various concentrations of dispersed graphene powder. The electrical conductivity of the samples was measured. In addition, terahertz transmission spectroscopy was used to retrieve the dielectric parameters of the samples. It was found that the electrical conductivity increased by several orders of magnitude with increasing graphene concentration, but even for the highest graphene concentration of 12 wt. %, the electrical conductivity was comparably low. Also, the measured electrical conductivity was several orders of magnitude too low to explain the measured absorption coefficient of the samples, which increased with increasing graphene concentration.

REFERENCES

[1] Sørgård, Trygve R., van Rheenen, Arthur D., and Haakestad, Magnus W., "Terahertz imaging of composite materials in reflection and transmission mode with a time-domain spectroscopy system", Terahertz, RF, Millimeter, and Submillimeter-Wave Technology and Application IX, 25 February 2016, 974714

[2] Web-of-Science search performed on 2. August 2018 with "graphene" as search phrase

[3] Keun Soo Kim, Yue Zhao, Houk Jang, Sang Yoon Lee, Jong Min Kim, Kwang S. Kim, Jong-Hyun Ahn, Philip Kim, Jae-Young Choi and Byung Hee Hong, "Large-scale pattern growth of graphene films for stretchable transparent electrodes", Nature 457 (2009) 706.

[4] Xiangping Li, Qiming Zhang, Xi Chen, and Min Gub , "Giant refractive-index modulation by two-photon reduction of fluorescent graphene oxides for multimode optical recording", Sci Rep.; 3: 2819 (2013)

[5] Melinda Y. Han, Barbaros Özyilmaz, Yuanbo Zhang, and Philip Kim "Energy band-gap engineering of graphene nanoribbons", Phys. Rev. Lett. 98, 206805 (2007).

[6] Gianluca Giovannetti, Petr A. Khomyakov, Geert Brocks, Paul J. Kelly, and Jeroen van den Brink "Substrate-induced band gap in graphene on hexagonal boron nitride: Ab initio density functional calculations", Phys. Rev. B 76, 073103 (2007).

[7] Xia, Fengnian, Farmer, Damon B., Lin, Yu-ming, and Avouris, Phaedon, "Graphene Field-Effect Transistors with high on/off current ratio and large transport band gap at room temperature", Nano Lett. 10, 715 (2010).

[8] University of Manchester (October 2013).

[9] Wu, Junbo, et al., “Organic Light-Emitting Diodes on solution-processed graphene transparent electrodes, ACS Nano 4 43 (2010).

[10] Liu C, Yu Z, Neff D, Zhamu A, Jang BZ, “Graphene-based supercapacitor with an ultrahigh energy density”, Nano Lett. 10, 4863 (2010).

[11] Chen W., Rakhia, R. B., and Alshareef, H. N.,” Capacitance enhancement of polyaniline coated curved-graphene supercapacitors in a redox-active electrolyte”, Nanoscale 5, 4134 (2013).

[12] Feifei Zhang, Jie Tang, Norio Shinya, Lu Chang Qin, “Hybrid graphene electrodes for supercapacitors of high energy density”, Chem. Phys. Lett. 584, 124 (2013).

[13] Jianyun Cao, et al., “High voltage asymmetric supercapacitor based on MnO2 and graphene electrodes”, J. Electroanal. Chem. 689, 201 (2013).

[14] Brownson, Dale. A. C., Kampouris, Dimitrios K., Banks, Craig E., “An overview of graphene in energy production and storage applications”. J. Power Sources 196 (11), 4873 (2011).

[15] Brownson, Dale. A. C, Banks, C. E.; “Fabricating graphene supercapacitors: highlighting the impact of surfactants and moieties”, Chem. Commun. 48 (10), 1425 (2012).

[16] Song W, Ji X, Deng W, Chen Q, Shen C, Banks CE., “Graphene ultracapacitors: structural impacts”, Phys. Chem. Chem. Phys. 15 (13), 4799 (2013).

[17] Randviir, Edward P., Brownson, Dale A. C., and Banks, Craig E., “A decade of graphene research: production, applications and outlook”, Materials Today, Vol. 17 (9), 426 (2014).

[18] Fanbin Menga, et al., “Graphene-based microwave absorbing composites: A review and prospective”, Composites Part B 137, 260–277 (2018).

[19] Ellrich, F., Weinland, T., Molter, D., Jonuscheit, J., and Beigang, R., "Compact fiber-coupled terahertz spectroscopy system pumped at 800 nm wavelength," *Review of Scientific Instruments*, vol. **82**, no. 5, 053102 (2011), 053102